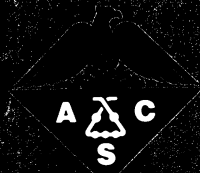


411-35

---

# JOURNAL OF THE AMERICAN CHEMICAL SOCIETY

---



# JOURNAL

## OF THE AMERICAN CHEMICAL SOCIETY®

VOLUME 110, NUMBER 14  
JULY 6, 1988

JACSAT 110(14) 4483-4876 (1988)  
ISSN 0002-7863

Registered in U.S. Patent and Trademark Office  
Copyright 1988 by the American Chemical Society

- 
- 1,2-Diphenylcycloalkenes: Electronic and Geometric Structures in the Gas Phase, Solution, and Solid State  
. . . Georg Hohlneicher,\* Martin Müller, Monika Demmer, Johann Lex, John H. Penn,\* Li-xian Gan, and Paul D. Loesel 4483 ■
- Rate Constants for Reactions in Viscous Media: Correlation between the Viscosity of the Solvent and the Rate Constant of the Diffusion-Controlled Reactions . . . . . Andres F. Olea and J. K. Thomas\* 4494
- Metal-Metal Bonding in  $(C_5H_5V)_2C_8H_8$ : A New Interpretation of ab Initio Results  
. . . Pierre Mougenot, Jean Demuyne, Marc Benard,\* and Charles W. Bauschlicher, Jr. 4503
- Bond-Stretch Isomerism in Transition-Metal Complexes  
. . . Yves Jean,\* Agusti Lledos, Jeremy K. Burdett,\* and Roald Hoffmann\* 4506
- Comparison of Direct and Through-Water Binding of Platinum Amines to the Phosphate Anion  
. . . M. Krauss,\* Harold Basch, and K. J. Miller 4517
- Ground States and Ionization Energies of  $Si_2H_6$ ,  $Si_3H_8$ ,  $Si_4H_{10}$ , and  $Si_5H_{12}$  . . . . . J. V. Ortiz\* and J. W. Mintmire 4522
- Conformational Studies by Dynamic NMR. 35. Structure, Conformation, and Stereodynamics of Hindered Naphthylamines  
. . . D. Casarini, E. Foresti, L. Lunazzi,\* and D. Macciantelli 4527 ■
- Homoallylic Chiral Induction in the Synthesis of 2,4-Disubstituted Tetrahydrofurans by Iodoetherification. Synthetic Scope and Chiral Induction Mechanism . . . . . M. Labelle,\* H. E. Morton, Y. Guindon,\* and J. P. Springer 4533 ■
- Resonance Raman Spectra of Dioxygen Adducts of Cobalt Porphyrins. Spectroscopic Manifestation of Vibrationally Coupled Dioxygen and Energy Matching of Interactive Modes  
. . . Leonard M. Proniewicz, Kazuo Nakamoto, and James R. Kincaid\* 4541
- Solid-State  $^{29}Si$  NMR and Infrared Studies of the Reactions of Mono- and Polyfunctional Silanes with Zeolite Y Surfaces  
. . . Thomas Bein,\* Robert F. Carver, Rodney D. Farlee, and Galen D. Stucky 4546
- Crystal Structures of  $(MeC_5H_4)_4U_2(\mu-NR)_2$ . Unsymmetrical Bridging,  $R = Ph$ , and Symmetrical Bridging,  $R = SiMe_3$ , Organoimide Ligands in Organoactinide Compounds . . . . . John G. Brennan, Richard A. Andersen,\* and Allan Zalkin 4554 ■
- Structure of the Cobalt(II)-"Capped" Porphyrin,  $Co(C_3-Cap)_3 \cdot 3CHCl_3$   
. . . John W. Sparapany, Maxwell J. Crossley, Jack E. Baldwin, and James A. Ibers\* 4559 ■
- Valence Trapping in Mixed-Valence  $Mn^{II}Mn^{III}$  Complexes of a Macrocyclic Binucleating Ligand  
. . . Hsiu-Rong Chang, Scott K. Larsen, Peter D. W. Boyd, Cortlandt G. Pierpont,\* and David N. Hendrickson\* 4565 ■
- Acid-Base Properties of Organic Solvents . . . . . Alessandro Bagno and Gianfranco Scorrano\* 4577 ■
- Borderline between E1cB and E2 Mechanisms. Elimination of HCl from Fluorene Derivatives . . . . . Alf Thibblin 4582
- Comparative Study of E2 and  $S_N2$  Reactions between Ethyl Halide and Halide Ion  
. . . Tsutomu Minato and Shinichi Yamabe\* 4586 ■
- Chiroptical Properties of Chiral Olefins  
. . . Aharon Gedanken,\* M. Duraisamy, Jiling Huang, J. Rachon, and H. M. Walborsky\* 4593
- Pentacoordinate Allylsilicates: Characterization and Highly Stereoselective Reaction with Aldehydes  
. . . Mitsuo Kira,\* Kazuhiko Sato, and Hideki Sakurai\* 4599
- Modeling Chemical Reactivity. 9. The Role of the Metal in Controlling the Stereochemistry of Nucleophilic Additions of Organometallic Reagents . . . . . S. D. Kahn,\* K. D. Dobbs, and W. J. Hehre\* 4602
- Intramolecular Hypervalent Sn-O Interaction. The Origin for Fixation of Six-Membered Carbocycles to the 1,3-Diaxial Conformer and for Stereoselective Osmylations  
. . . Masahito Ochiai,\* Shigeru Iwaki, Tatsuzo Ukita, Yoshiki Matsuura, Motoo Shiro, and Yoshimitsu Nagao\* 4606 ■
- Asymmetric Tandem Addition to Chiral 1- and 2-Substituted Naphthalenes. Application to the Synthesis of (+)-Phylltetralin  
. . . A. I. Meyers,\* Gregory P. Roth, Denton Hoyer, Bruce A. Barner, and Dominique Laucher 4611 ■
- Face Selectivity in Diels-Alder Reactions of Chiral Dienes Containing Allylic Substituents  
. . . Matthew J. Fisher, Warren J. Hehre, Scott D. Kahn, and Larry E. Overman\* 4625 ■
- The Charge Alternation Concept: Application to Cyclic Conjugated Doubly Charged Systems  
. . . Yoram Cohen, Joseph Klein,\* and Mordecai Rabinovitz\* 4634

- Electrophilic Additions to 3-C-[(Methoxycarbonyl)methyl]-3-deoxy-D-ribofuranose Enolates: A Case of Unusually Efficient Non-Chelate-Enforced Chirality Transfer . . . . . **Johann Mulzer,\* Ulrich Steffen, Ludwig Zorn, Christian Schneider, Elmar Weinhold, Winfried Münch, Rainer Rudert, Peter Luger, and Hans Hartl** 4640 ■
- Photolyses of Organocobaloxime Having Alkyl and (Alkylthio)carbonyl Groups on the  $\beta$ -Position. A Radical Reaction Involving the Thioester Group . . . . . **Masaru Tada,\* Tatsuya Nakamura, and Mitsuhiro Matsumoto** 4647
- Highly Diastereofacial Selective Chelation of a Phosphite-Containing  $\alpha,\beta$ -Unsaturated Ketone System to the  $\text{Fe}(\text{CO})_2$  Group . . . . . **Wei-Yuan Zhang, Dennis J. Jakiela, André Maul, Christopher Knors, Joseph W. Lauher, Paul Helquist,\* and Dieter Enders** 4652 ■
- Chemistry of Amphotericin B. Degradation Studies and Preparation of Amphoteronolide B . . . . . **K. C. Nicolaou,\* T. K. Chakraborty, Y. Ogawa, R. A. Daines, N. S. Simpkins, and G. T. Furst** 4660
- Total Synthesis of Amphoteronolide B and Amphotericin B. 1. Strategy and Stereocontrolled Construction of Key Building Blocks . . . . . **K. C. Nicolaou,\* R. A. Daines, J. Uenishi, W. S. Li, D. P. Papahatjis, and T. K. Chakraborty** 4672
- Total Synthesis of Amphoteronolide B and Amphotericin B. 2. Total Synthesis of Amphoteronolide B . . . . . **K. C. Nicolaou,\* R. A. Daines, T. K. Chakraborty, and Y. Ogawa** 4685
- Total Synthesis of Amphotericin B. 3. The Final Stages . . . . . **K. C. Nicolaou,\* R. A. Daines, Y. Ogawa, and T. K. Chakraborty** 4696
- Organic Ligand-Receptor Interactions between Cucurbituril and Alkylammonium Ions . . . . . **William L. Mock\* and Neng-Yang Shih** 4706
- Ab Initio Calculations of the Olefin Strain Energies of Some Pyramidalized Alkenes . . . . . **David A. Hrovat and Weston Thatcher Borden\*** 4710 ■
- The Three-Component Coupling Synthesis of Prostaglandins . . . . . **M. Suzuki, A. Yanagisawa, and R. Noyori\*** 4718
- Triply Convergent Synthesis of (-)-Prostaglandin  $\text{E}_2$  Methyl Ester . . . . . **Carl R. Johnson\* and Thomas D. Penning** 4726 ■
- Enantioselective Synthesis through Microbial Oxidation of Arenes. 1. Efficient Preparation of Terpene and Prostanoid Synthons . . . . . **Tomas Hudlicky,\* Hector Luna, Graciela Barbieri, and Lawrence D. Kwart** 4735
- Enantioselective Total Synthesis of (+)-12,13-Epoxytrichothec-9-ene and Its Antipode . . . . . **Duy H. Hua,\* S. Venkataraman, Roch Chan-Yu-King, and Joseph V. Paukstelis** 4741
- Gas-Phase Determination of the Geometric Requirements of the Silicon  $\beta$ -Effect. Photoelectron and Penning Ionization Electron Spectroscopic Study of Silylthiiranes and -oxiranes. Synthesis and Chemistry of *trans*-2,3-Bis(trimethylsilyl)thiirane . . . . . **Eric Block,\* Andrew J. Yencha,\* Mohammad Aslam, Venkatachalam Eswarakrishnan, Jianzhi Luo, and Akinobu Sano** 4748 ■
- One-Pot, Four-Component Annulations: Flexible and Simple Syntheses of Unsaturated Macrolides and of Substituted Aromatics and Heteroaromatics . . . . . **Gary H. Posner,\* Kevin S. Webb, Edward Asirvatham, Sang-sup Jew, and Alessandro Degl'Innocenti** 4754
- Totally Stereoselective Additions to 2,6-Disubstituted 1,3-Dioxin-4-ones (Chiral Acetoacetic Acid Derivatives). Synthetic and Mechanistic Aspects of Remote Stereoselectivity . . . . . **Dieter Seebach,\* Jürg Zimmermann, Urs Gysel, Regula Ziegler, and Tae-Kyu Ha** 4763 ■
- Facilitation of Electrochemical Oxidation of Dialkyl Sulfides Appended with Neighboring Carboxylate and Alcohol Groups . . . . . **Richard S. Glass,\* Amorn Petsom, Massoud Hojjatie, Brian R. Coleman, John R. Duchek, Jacob Klug, and George S. Wilson\*** 4772 ■
- Chiral and Achiral Formamidines in Synthesis. The First Asymmetric Route to (-)-Yohimbone and an Efficient Total Synthesis of ( $\pm$ )-Yohimbone . . . . . **A. I. Meyers,\* Donald B. Miller, and Franklin H. White** 4778 ■
- Vinylolithium Cyclizations with Unactivated Alkenes as Internal Electrophiles: Stereoselective Formation of Substituted Methylenecyclopentanes . . . . . **A. Richard Chamberlin,\* Steven H. Bloom, Laura A. Cervini, and Christopher H. Fotsch** 4788 ■
- Total Synthesis of ( $\pm$ )- $N^2$ -(Phenylsulfonyl)-CPI, ( $\pm$ )-CC-1065, (+)-CC-1065, *ent*-(-)-CC-1065, and the Precise, Functional Agents ( $\pm$ )-CPI-CDPI<sub>2</sub>, (+)-CPI-CDPI<sub>2</sub>, and (-)-CPI-CDPI<sub>2</sub> [( $\pm$ )-(3*bR*\*,4*aS*\*)-, (+)-(3*bR*,4*aS*)-, and (-)-(3*bS*,4*aR*)-Deoxy-CC-1065] . . . . . **Dale L. Boger\* and Robert S. Coleman** 4796 ■
- Acromelic Acids A and B. Potent Neuroexcitatory Amino Acids Isolated from *Clitocybe acromelalga* . . . . . **Katsuhiko Konno, Kimiko Hashimoto, Yasufumi Ohfune, Haruhisa Shirahama,\* and Takeshi Matsumoto** 4807
- A New Route to the Prostaglandin Skeleton via Radical Alkylation. Synthesis of 6-Oxoprostaglandin  $\text{E}_1$  . . . . . **Takeshi Toru,\* Yoshio Yamada, Toshio Ueno, Etsuro Maekawa, and Yoshio Ueno** 4815 ■
- Enzymatic Cyclization of Hydroxylated Surrogate Squalenoids with Bakers' Yeast . . . . . **Julio C. Medina and Keith S. Kyler\*** 4818

## COMMUNICATIONS TO THE EDITOR

- A Sulfur-Mediated Total Synthesis of Zygospurin E . . . . . **E. Vedejs,\* J. D. Rodgers, and S. J. Wittenberger** 4822 ■
- Highly Efficient Synthesis of Carbacyclin Analogue. Stereospecific Synthesis of Aryl-Substituted Exocyclic Olefin . . . . . **Mikiko Sodeoka, Shoji Satoh, and Masakatsu Shibasaki\*** 4823 ■

- Diastereoselective Photodeconjugation of  $\alpha,\beta$ -Unsaturated Esters  
 . . . **Reza Mortezaei, Djamsah Awandi, Françoise Henin, Jacques Muzart,\* and Jean-Pierre Pete\*** 4824
- High Diastereofacial Selectivity in Nucleophilic Additions to Chiral Acylsilanes  
 . . . **Masahisa Nakada, Yasuharu Urano, Susumu Kobayashi, and Masaji Ohno\*** 4826 ■
- Pentacyclo[5.1.0.0<sup>2,4</sup>.0<sup>3,5</sup>.0<sup>6,8</sup>]octane (Octabisvalene) . . . **Christoph Rücker\* and Björn Trupp** 4828
- ClO<sub>2</sub> Oxidation of Amines: Synthetic Utility and a Biomimetic Synthesis of Elaecarpidine  
 . . . **Chien-Kuang Chen, Alfred G. Hortmann,\* and Mohammad R. Marzabadi** 4829
- A New Method for the Formation of Nitrogen-Containing Ring Systems via the Intramolecular Photocycloaddition of  
 Vinylogous Amides. A Synthesis of Mesembrine . . . **Jeffrey D. Winkler,\* Cheryl L. Muller, and Robert D. Scott** 4831 ■
- On the Tautomerism of Dihydropyrimidines: The Influence of the 2- and 5-Substituents on the Observation of Tautomers  
 . . . **Hidetsura Cho,\* Takashi Iwashita, Masaru Ueda, Akira Mizuno, Kosei Mizukawa, and Mikiko Hamaguchi** 4832 ■
- Effects of BF<sub>3</sub>·Et<sub>2</sub>O on Higher Order Organocuprate Reactions: Substrate Activation or Cuprate Modification?  
 . . . **Bruce H. Lipshutz,\* Edmund L. Ellsworth, and Teruna J. Siahaan** 4834 ■
- Antibody Catalysis of Bimolecular Amide Formation . . . **K. D. Janda, R. A. Lerner,\* and A. Tramontano\*** 4835
- Ovothiols as Biological Antioxidants. The Thiol Groups of Ovithiol and Glutathione Are Chemically Distinct  
 . . . **Tod P. Holler and Paul B. Hopkins\*** 4837
- A Versatile Route to Diastereomeric Tungstenocene Complexes Containing Chiral Metal Centers  
 . . . **John P. McNally, David Glueck, and N. John Cooper\*** 4838 ■
- Macrolide Biosynthesis. 5. Intact Incorporation of a Chain-Elongation Intermediate into Nargenicin  
 . . . **David E. Cane\* and Walter R. Ott** 4840
- An Antibody-Catalyzed Claisen Rearrangement  
 . . . **D. Y. Jackson, J. W. Jacobs, R. Sugawara, S. H. Reich, P. A. Bartlett,\* and P. G. Schultz\*** 4841 ■
- From Twisted to Folded Ethylenes . . . **Agha Zul-Qarnain Khan and Jan Sandström\*** 4843
- X-ray Structures of Threaded Et<sub>2</sub>Mg(18-crown-6) and Et<sub>2</sub>Zn(18-crown-6)  
 . . . **Anthony D. Pajerski, Gretchen L. BergStresser, Masood Parvez, and Herman G. Richey, Jr.\*** 4844 ■
- X-ray Structure of (1,3-Xylyl-18-crown-5)diphenylmagnesium: An Organometallic Rotaxane . . . **Peter R. Markies,  
 Tateo Nomoto, Otto S. Akkerman, Friedrich Bickelhaupt,\* Wilberth J. J. Smeets, and Anthony L. Spek** 4845 ■
- Bis(2,3,4,6,7- $\eta^5$ -bicyclo[3.2.2]nona-2,6,8-trien-4-yl)iron, a Ferrocene Analogue with Separated Allyl and Olefin Systems  
 . . . **Janet Blümel, Frank H. Köhler,\* and Gerhard Müller** 4846 ■
- Modification of Photochemical Reactivity by Zeolites: Norrish Type I and Type II Reactions of Benzoin Derivatives  
 . . . **D. R. Corbin, D. F. Eaton, and V. Ramamurthy\*** 4848
- ( $\mu$ -NO)<sub>2</sub>[Co( $\eta^5$ -C<sub>5</sub>H<sub>5</sub>)<sub>2</sub>] Is Not Paramagnetic . . . **David J. Berg and Richard A. Andersen\*** 4849
- Mycalamide A, an Antiviral Compound from a New Zealand Sponge of the Genus *Mycale*  
 . . . **Nigel B. Perry, John W. Blunt,\* Murray H. G. Munro,\* and Lewis K. Pannell** 4850
- Isolation and Structure Elucidation of Onnamide A, a New Bioactive Metabolite of a Marine Sponge, *Theonella* sp.  
 . . . **Shinichi Sakemi, Toshio Ichiba, Shigeo Kohmoto, Gabriel Saucy, and Tatsuo Higa\*** 4851 ■
- Synthesis and Physical Properties of a Dinuclear Tantalum-Cobalt Radical with Spin Localized at One Metal Center  
 . . . **Karen I. Goldberg and Robert G. Bergman\*** 4853 ■
- A Carbon-Carbon Bond Cleavage Reaction of Carbon Suboxide at a Metal Center. Synthesis and Structural Characterization  
 of WCl<sub>2</sub>(CO)(PMePh<sub>2</sub>)<sub>2</sub>{C,C': $\eta^2$ -C(O)CPMePh<sub>2</sub>} . . . **Adam K. List, Gregory L. Hillhouse,\* and Arnold L. Rheingold\*** 4855 ■
- Dercitin, a New Biologically Active Acridine Alkaloid from a Deep Water Marine Sponge, *Dercitus* sp.  
 . . . **Geewananda P. Gunawardana, Shigeo Kohmoto, Sarath P. Gunasekera, Oliver J. McConnell,\* and Frank E. Koehn** 4856 ■
- Synthetic Studies on Arene-Olefin Cycloadditions. 10. A Concise, Stereocontrolled Total Synthesis of ( $\pm$ )-Laurenene  
 . . . **Paul A. Wender,\* Thomas W. von Geldern, and Barry H. Levine** 4858 ■
- An Ethylene Complex of Vanadium: Synthesis, Structure, and Reactivity of  
 Cyclopentadienyl-bis(trimethylphosphine)(ethylene)vanadium(I) . . . **Bart Hessen, Auke Meetsma, and Jan H. Teuben\*** 4860 ■
- Stereochemistry of the Biosynthesis of *sn*-2,3-*O*-Diphytanyl Glycerol, Membrane Lipid of Archaeobacteria  
*Halobacterium halobium*  
 . . . **Katsumi Kakinuma,\* Masahiro Yamagishi, Yoshinori Fujimoto, Nobuo Ikekawa, and Tairo Oshima** 4861
- [S<sub>4</sub>Cd<sub>17</sub>(SPh)<sub>28</sub>]<sup>2-</sup>, the First Member of a Third Series of Tetrahedral [S<sub>w</sub>M<sub>x</sub>(SR)<sub>y</sub>]<sup>z-</sup> Clusters  
 . . . **Garry S. H. Lee, Don C. Craig, Ida Ma, Marcia L. Scudder, Trevor D. Bailey, and Ian G. Dance\*** 4863 ■
- A Novel Mechanism of Glycoside Anomerization . . . **Leise A. Berven, David H. Dolphin, and Stephen G. Withers\*** 4864
- Cyclic Conjugated Eneidyne Related to Calicheamicins and Esperamicins: Calculations, Synthesis, and Properties  
 . . . **K. C. Nicolaou,\* G. Zuccarello, Y. Ogawa, E. J. Schweiger, and T. Kumazawa** 4866 ■

Novel Chemistry of Dithiatopazine . . . . .	K. C. Nicolaou,* C.-K. Hwang, S. DeFrees, and N. A. Stylianides	4868 ■
Carbon Dioxide Activation: Thermodynamics of CO <sub>2</sub> Binding and the Involvement of Two Cobalt Centers in the Reduction of CO <sub>2</sub> by a Cobalt(I) Macrocycle . . . . .	Etsuko Fujita,* David J. Szalda, Carol Creutz,* and Norman Sutin*	4870 ■
A Novel Molybdenum(0) Dinitrogen Complex Containing Crown Thioether as the Sole Auxiliary Ligand: <i>trans</i> -Mo(N <sub>2</sub> ) <sub>2</sub> Me <sub>8</sub> [16]aneS <sub>4</sub> (Me <sub>8</sub> [16]aneS <sub>4</sub> = 3,3,7,7,11,11,15,15-Octamethyl-1,5,9,13-tetrathiacyclohexadecane) . . . . .	Toshikatsu Yoshida,* Tomohiro Adachi, Manabu Kaminaka, Tatsuo Ueda, and Taiichi Higuchi	4872 ■

## ADDITIONS AND CORRECTIONS

On the Origin of Proximity Effects on Reactivity: A Modified MM2 Model for the Rates of Acid-Catalyzed Lactonizations of Hydroxy Acids . . . . .	Andrea E. Dorigo and K. N. Houk*	4874
--	----------------------------------	------

## BOOK REVIEWS

Physical Methods of Chemistry. Second Edition. Volume IIIA. Determination of Chemical Composition and Molecular Structure, Part A . . . . .	Reviewed by Norman E. Heimer	4874
Heterogeneous Catalysis: Principles and Applications. Second Edition. By G. C. Bond . . . . .	Reviewed by Allan Hydorn	4874
The Alkaloids. Volume 27 . . . . .	Reviewed by Scott L. Dax	4874
Thin Layer Chromatography. By Richard J. Hamilton and Shiela Hamilton . . . . .	Reviewed by David C. Locke	4875
Atomic Absorption and Emission Spectroscopy. By E. Metcalfe . . . . .	Reviewed by R. Kenneth Marcus	4875
Topics in Current Chemistry. No. 139. Organic Geo- and Cosmochemistry . . . . .	Reviewed by Stan Neely	4875
Pseudopotential Theory of Atoms and Molecules. By L. Szasz . . . . .	Reviewed by Michel Pelissier	4876
Studies in Physical and Theoretical Chemistry. Volume 49. Metallic Superlattices, Artificial Structured Materials . . . . .	Reviewed by Michael L. Norton	4876
Methods in Enzymology. Volume 127. Biomembranes. Part O. Protons and Water: Structure and Translocation. Volume 128. Plasma Lipoproteins. Part A. Preparation, Structure, and Molecular Biology. Volume 153. Recombinant DNA. Part D. Volume 155. Recombinant DNA. Part F . . . . .		4876
Organic Electronic Spectral Data. Volume XXIII . . . . .		4876

■ Supplementary material for this paper is available separately (consult the masthead page for ordering information); all supplementary material except structure factor tables will also appear following the paper in the microfilm edition of this journal.

\* In papers with more than one author, the asterisk indicates the name of the author to whom inquiries about the paper should be addressed.

# Solid-State $^{29}\text{Si}$ NMR and Infrared Studies of the Reactions of Mono- and Polyfunctional Silanes with Zeolite Y Surfaces

Thomas Bein,<sup>\*,†,‡</sup> Robert F. Carver,<sup>‡</sup> Rodney D. Farlee,<sup>‡</sup> and Galen D. Stucky<sup>‡</sup>

Contribution No. 4190 from the Central Research and Development Department, E. I. du Pont de Nemours and Company, Experimental Station, Wilmington, Delaware 19898, and the Department of Chemistry, University of California, Santa Barbara, California 93106. Received February 26, 1987

**Abstract:** The combined use of  $^{29}\text{Si}$  magic-angle spinning NMR spectroscopy and in situ infrared techniques allows for the first time the determination of the intrazeolitic reaction products and details of the interaction of various silanes with zeolitic protons in HY zeolite. Alkoxy groups at  $\text{Me}_3\text{SiOMe}$  and  $\text{MeSi(OMe)}_3$  are readily lost to form hydroxy groups and then siloxane bridges to the zeolite framework. At elevated temperatures, alkyl groups are also split off from the silane, and more highly substituted siloxane species are generated which are anchored to the framework via two siloxane bridges. Chloro groups at trimethylchlorosilane are rapidly hydrolyzed by the surface hydroxy groups, and the resulting products follow the reaction pattern of the alkoxy silanes. Hexamethyldisilazane and trimethylsilane do not react irreversibly with the zeolite hydroxyls at 295 K but are as reactive as other silanes at 473 K. A major product with these silanes shows a unique NMR shift at about +40 ppm and is assigned to a Lewis acid or strongly hydrogen-bonded association of the anchored silicon species with a framework metal. Most of the reactions are more complex than those of halosilanes with the terminal hydroxyls of silica, indicating the extreme reactivity of bridged hydroxyl groups in zeolites.

The chemical modification of zeolites has attracted considerable attention since these crystalline porous materials were introduced several decades ago. Ion exchange by transition metals and ammonium ions plays a major role to control catalytic and acidic properties. The complex zeolite structure is, however, by far not limited to modifications by these techniques, and recent work has focused on tailoring the hydrophobicity, adjusting the pore sizes, or specifically poisoning certain catalytic functions of the zeolite surface.

The intention of this study is to explore the possibility of "anchoring" certain molecules to the internal surface of the zeolite pore system. If reactions of this kind could be controlled, a general means would be available for the synthesis of fixed ligands, acids, or other functional groups in the pore system. Silanes represent a well-known class of reagents for the modification of oxide surfaces, and a number of studies deal with surface reactions of silanes with zeolites.<sup>1-14</sup>

While the reactivity of polyfunctional silanes with zeolites has been established, only limited attempts have been undertaken to characterize the systems obtained by the various treatments. In this study, a combination of solid-state magic-angle spinning NMR (MAS NMR) and in situ infrared spectroscopy has been employed to elucidate the chemistry of silanes in the pore system of acid zeolites. MAS NMR has recently been used for detailed studies on related reactions of silanes with the terminal hydroxyls of amorphous silica.<sup>15-23</sup>

Infrared spectroscopy as a complementary technique contributes to the understanding of acid-base chemistry of oxide surfaces and has been applied to differentiate between the reactivity of geminal and single silica hydroxyls toward hexamethyldisilazane and methyltrimethoxysilane.<sup>24,25</sup>

## Experimental Section

**1. Materials.** Trimethylmethoxysilane, methyltrimethoxysilane, trimethylchlorosilane, and hexamethyldisilazane (Strem Chemicals) were stored over sieve 4A without further purification. Gaseous trimethylsilane (Petrarch Systems) was used without purification.  $\text{NH}_4\text{Y}$  zeolite with the composition  $\text{Na}_8(\text{NH}_4)_{47}\text{Al}_{55}\text{Si}_{137}\text{O}_{384}n\text{H}_2\text{O}$  was obtained from Linde (LZ-Y62). Prior to use, the ammonium form of the zeolite was degassed by heating at a rate of 2 K/min to 670 K and maintained at 670 K for 12 h under  $10^{-5}$  Torr to yield the dry acid form (HY).

**2. Methods.** Samples for solid-state NMR experiments were prepared as follows. Batches of dry HY (ca. 500 mg) were weighed into a small

quartz holder, introduced into a tubular quartz reactor, and evacuated at a greaseless vacuum line ( $10^{-5}$  Torr) for 30 min. A degassed and frozen vial containing the silane was allowed to warm to 273 K and dosed manometrically onto the zeolite. After equilibrating for 120 min at 295 K, the sample was evacuated for 30 min, and weight changes were recorded in the drybox. The calculated loading (molecules of silanes per superpage, X/SC) is listed for each sample in the corresponding figure caption, based on equivalents of physisorbed silane. Heat treatments were done in the same reactor under vacuum, or under the vapor pressure of the silane, with a heating rate of 1 K/min. With trimethylsilane, an excess was dosed on the zeolite at a pressure of 50 Torr.

The  $^{29}\text{Si}$  NMR spectra were obtained at 59.6 MHz on a Bruker CXP-300 instrument. Andrews type rotors were filled with ca. 200 mg of sample in the drybox and introduced into the NMR probe in a glovebag under flowing nitrogen. All spectra were obtained with magic-angle spinning (MAS) and cross-polarization (CP). The rotor was driven by dry nitrogen gas to obtain spinning rates between 2 and 4 kHz.

- (1) Geismar, G.; Westphal, U. Z. *Anorg. Allg. Chem.* **1982**, *484*, 131.
- (2) McAteer, J. C.; Rooney, J. J. In *Adv. Chem. Ser.* **1973**, *121*, 258.
- (3) Barrer, R. M.; Trombe, J. C. *J. Chem. Soc., Faraday Trans. 1* **1978**, *74*, 2786.
- (4) Barrer, R. M.; Trombe, J. C. *J. Chem. Soc., Trans. 1* **1978**, *74*, 2798.
- (5) Barrer, R. M.; Vansant, E. F.; Peeters, G. *J. Chem. Soc., Faraday Trans. 1* **1978**, *74*, 1871.
- (6) Thijs, A.; Peeters, G.; Vansant, E. F.; Verhaert, I. *J. Chem. Soc., Faraday Trans. 1* **1983**, *79*, 2835.
- (7) Thijs, A.; Peeters, G.; Vansant, E. F.; Verhaert, I. *J. Chem. Soc., Faraday Trans. 1* **1983**, *79*, 2821.
- (8) Niwa, M.; Murakami, Y. *Hyomen* **1984**, *22*, 319.
- (9) Rodewald, P. G. U.S. Patent 4 402 867, 1983.
- (10) Kerr, G. T. U.S. Patent 3 682 996, 1972.
- (11) Gortsema, F. P.; Lok, B. M. Eur. Pat. Appl. 0 100 544, 1983.
- (12) Kittelmann, U.; Diehl, M.; Bergmann, R.; Stadtmüller, G. U.S. Patent 4 454 056, 1984.
- (13) Campbell, T. C. et al., U.S. Patent 4 216 125, 1980.
- (14) Hertzberg, E. P., et al., U.S. Patent 4 138 363, 1979.
- (15) Sindorf, D. W.; Maciel, G. E. *J. Phys. Chem.* **1983**, *87*, 5516.
- (16) Sindorf, D. W.; Maciel, G. E. *J. Am. Chem. Soc.* **1983**, *105*, 1487.
- (17) Sindorf, D. W.; Maciel, G. E. *J. Phys. Chem.* **1982**, *86*, 5208.
- (18) Maciel, G. E.; Sindorf, D. W.; Bartuska, V. J. *J. Chromatogr.* **1981**, *205*, 438.
- (19) Sindorf, D. W.; Maciel, G. E. *J. Am. Chem. Soc.* **1981**, *103*, 4263.
- (20) Maciel, G. E.; Sindorf, D. W. *J. Am. Chem. Soc.* **1980**, *102*, 7606.
- (21) Kohler, J.; Chase, D. B.; Farlee, R. D.; Vega, A. J.; Kirkland, J. J. *J. Chromatogr.* **1986**, *352*, 275.
- (22) Miller, M. L.; Linton, R. W.; Maciel, G. E.; Hawkins, B. L. *J. Chromatogr.* **1985**, *319*, 9.
- (23) Bayer, E.; Albert, K.; Reiners, J.; Nieder, M.; Müller, D. *J. Chromatogr.* **1983**, *264*, 197.
- (24) Hertl, W.; Hair, M. L. *J. Phys. Chem.* **1971**, *76*, 2181.
- (25) Hertl, W. *J. Phys. Chem.* **1968**, *72*, 1248.

<sup>†</sup> Present address: Department of Chemistry, University of New Mexico, Albuquerque, NM 87131.

<sup>‡</sup> Du Pont.

<sup>‡</sup> UC Santa Barbara.

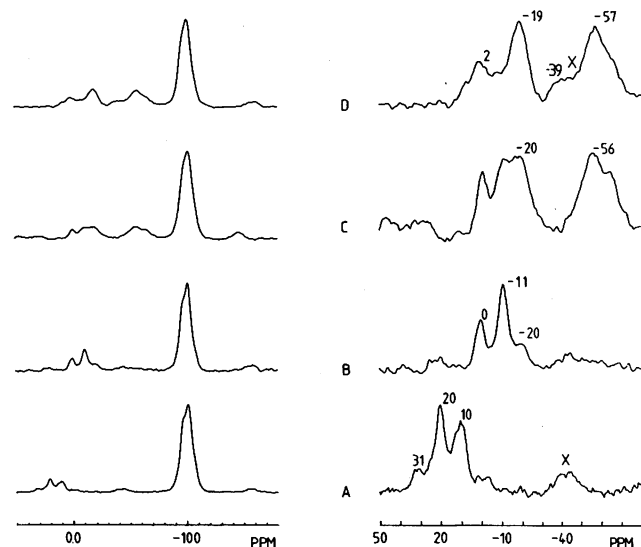


**Figure 1.**  $^{29}\text{Si}$  CP-MAS NMR spectra of trimethylmethoxysilane chemisorbed on dehydrated HY zeolite. X denotes spinning sidebands of the zeolite framework resonances. (A) Equilibrated for 120 min at 295 K, degassed for 30 min (2.4 equiv per supercage, 2.4/SC); (B) degassed at 403 K for 180 min; (C) degassed at 523 K for 12 h; and (D) equilibrated at 473 K for 120 min, degassed for 30 min (2.4/SC).

Previously reported studies of structurally similar species on derivatized silica have defined conditions which yield quantitative spectra,<sup>21</sup> 10 ms cross-polarization, followed by 20 to 60 ms  $^1\text{H}$  decoupling, was used for all spectra reported here. 1000 to 8000 scans were acquired to obtain adequate signal-to-noise ratio. The quantitative accuracy of this CP experiment was verified in selected samples by Bloch decay experiments, employing a  $7\ \mu\text{s}$   $90^\circ$  pulse and 10 s recycle delay. Chemical shifts were referenced to  $\text{Me}_4\text{Si}$ , using external hexamethyltrisiloxane in  $\text{CDCl}_3$  ( $-9.2$  ppm) as secondary reference. No significant oxidation of the silanes was observed during the NMR experiments.

In situ infrared experiments were done with self-supporting zeolite wafers ( $5\ \text{mg}/\text{cm}^2$ ) compacted at  $100\ \text{kg}/\text{cm}^2$ , in a controlled-atmosphere cell with  $\text{CaF}_2$  windows connected to a Nicolet 5DXB FT-IR spectrometer. Sample treatment was similar to that of the NMR samples, with the exception of shorter temperature cycles.

In order to facilitate a comparison of relative amounts of surface silyl species, the relative intensities of all  $^{29}\text{Si}$  resonances observed downfield from the bulk zeolite are given in mole percentages. This is based upon the assumption that negligible amounts of the silanes have been oxidized to  $\text{Si}(\text{OX})_4$  species which would be obscured by the bulk zeolite resonance.

## Results and Discussion

**Trimethylmethoxysilane.**  $^{29}\text{Si}$  MAS NMR spectra of HY loaded with  $\text{Me}_3\text{SiOMe}$  vapor are shown in Figure 1, A–D left. The major resonances are due to silicon in the zeolite framework having one Al and three Si neighbors at  $-98$  ppm and having four Si neighbors at  $-101.5$  ppm. Throughout this study, the chemical shifts of these resonances are unchanged. Slight variations in the relative intensities of these resonances are observed and reflect differences in the spin–lattice relaxation times of the framework Si sites in these dehydrated zeolites. The region of interest in this work spans the chemical shifts of silanes and siloxanes and is expanded in Figures 1, A–D right.

The  $^{29}\text{Si}$  NMR chemical shift is a powerful tool for identifying various surface sites. Of interest in this work are the chemical shifts of silicon bonded to Me, OMe, OH, and Cl groups and bonded to the silica or aluminosilicate surface by a bridging oxygen, as in a disiloxane (here denoted OSi). From the large body of relevant data available in the literature<sup>26,27,29</sup> chemical

**Table I.**  $^{29}\text{Si}$  Chemical Shifts of Substituted Methylsilanes

molecule or site	shift <sup>a</sup>	molecule or site	shift <sup>a</sup>
Monosubstituted			
$\text{Me}_3\text{SiCl}$	+30 <sup>b</sup>	$\text{Me}_3\text{SiOSi}$	+8 <sup>d</sup>
$\text{Me}_3\text{SiOMe}$	+18 <sup>b</sup>	$\text{Me}_3\text{SiH}$	-16 <sup>b</sup>
$\text{Me}_3\text{SiOH}$	+17 <sup>c</sup>		
Disubstituted			
$\text{Me}_2\text{SiCl}_2$	+32 <sup>b</sup>	$\text{Me}_2\text{Si}(\text{OH})\text{OSi}$	-12 <sup>d</sup>
$\text{Me}_2\text{Si}(\text{Cl})\text{OSi}$	+2 <sup>d</sup>	$\text{Me}_2\text{Si}(\text{OSi})_2$	-14 <sup>d</sup>
$\text{Me}_2\text{Si}(\text{OMe})_2$	-2 <sup>b</sup>		
Trisubstituted			
$\text{MeSiCl}_3$	+12 <sup>b</sup>	$\text{MeSi}(\text{OH})_2(\text{OSi})$	-42 <sup>d</sup>
$\text{MeSi}(\text{Cl})_2\text{OSi}$	-14 <sup>d</sup>	$\text{MeSi}(\text{OH})(\text{OSi})_2$	-52 <sup>d</sup>
$\text{MeSi}(\text{Cl})(\text{OSi})_2$	-38 <sup>d</sup>	$\text{MeSi}(\text{OMe})(\text{OSi})_2$	-58 <sup>c</sup>
$\text{MeSi}(\text{Cl})(\text{OH})(\text{OSi})$	-29 <sup>d</sup>	$\text{MeSi}(\text{OSi})_3$	-62 <sup>d</sup>
$\text{MeSi}(\text{OMe})_3$	-41 <sup>b</sup>		
Quaternary			
$\text{Si}(\text{OMe})_4$	-79 <sup>b,e</sup>	$\text{Si}(\text{OH})_3(\text{OSi})$	-83 <sup>g,h</sup>
$\text{Si}(\text{OMe})_3(\text{OSi})$	-86 <sup>e</sup>	$\text{Si}(\text{OH})_2(\text{OSi})_2$	-92 <sup>h,i</sup>
$\text{Si}(\text{OMe})_2(\text{OSi})_2$	-94 <sup>e</sup>	$\text{Si}(\text{OH})(\text{OSi})_3$	-104 <sup>h,j</sup>
$\text{Si}(\text{OMe})(\text{OSi})_3$	-104 <sup>e</sup>	$\text{Si}(\text{OSi})_4$	-112 <sup>h,j</sup>
$\text{Si}(\text{OH})_4$	-74 <sup>f</sup>		

<sup>a</sup> In ppm relative to  $\text{Me}_4\text{Si}$ . <sup>b</sup> Table 10.1, p 313, in ref 29. <sup>c</sup> Predicted using additive substituent effects from data in ref 29, following the method outlined in ref 27 as further discussed in the text. <sup>d</sup> Reference 27. <sup>e</sup> Reference 31. <sup>f</sup> Farlee, R. D.; Concannon, T. P., unpublished work. Similar values have been reported elsewhere (ref 28 and 30). <sup>g</sup> Average value for disilicates. <sup>h</sup> Analogous sites in silicates exhibit chemical shifts covering a substantial range (ref 32) depending on the average substituent electronegativity and Si–O–Si angle (ref 28). <sup>i</sup> These are typical values for silica (ref 21 and 27). <sup>j</sup> Q4 sites in zeolites and tectosilicates span a considerable range and can be predicted from the number of Al neighbors and average Si–O–T (T = Si, Al) angle (ref 33).

shifts of essentially all the possible products with the species of interest in this work can be compiled (Table I). It is important to note that mono-, di-, and trisubstitution are resolved in well-defined  $^{29}\text{Si}$  chemical shift regions.

It should be noted that it appears that a small but consistent downfield shift is observed in the solid state relative to solution. Sindorf and Maciel<sup>27</sup> report an average “solid-state  $^{29}\text{Si}$  chemical shift” difference of +7 ppm for trimethylsilyl groups bonded to a silica surface, relative to their shift in solution. We find this value to vary between +2 and +7 ppm in the species studied here. This shift is not included in those data reported in Table I which were measured in solution.

The chemical shifts of discrete alkyl monosilicate species are not available because of their instability toward rapid condensation to higher silicates. However, one would expect that the shifts for the series  $\text{Si}(\text{OH})_n(\text{OMe})_{4-n}$  would all lie between  $-79$  ppm ( $n = 0$ )<sup>29,32</sup> and  $-74$  ppm ( $n = 4$ )<sup>29,31</sup> if the substituent effects are assumed to be linearly additive.

The coverage of silicas can be calculated directly from the areas of the  $\text{Si}(\text{OH})_2(\text{OSi})_2$ ,  $\text{Si}(\text{OH})(\text{OSi})_3$ , and  $\text{Me}_3\text{Si}(\text{OSi})$  resonances in  $^{29}\text{Si}$  CP-MAS spectra.<sup>15,17,20,21</sup> In zeolite Y, these effects are masked by signal from the bulk zeolite and cannot be differentiated from the external surface.

If dehydrated HY zeolite is saturated with vapor of  $\text{Me}_3\text{SiOMe}$  at 295 K, three new silicon species at 31, 20, and 10 ppm are observed in the  $^{29}\text{Si}$  MAS NMR of the zeolite (Figure 1A). The species at 20 ppm (45 mol %) can be assigned either to the starting silane (17.7 ppm in solution) or to the hydrolysis product,  $\text{Me}_3\text{SiOH}$ , which has a predicted shift of 17 ppm (see Table I). These observations, including assignments, are summarized in Table II.

(26) Williams, E. A. *Annu. Rep. NMR Spectrosc.* **1983**, *15*, 235.

(27) Sindorf, D. W.; Maciel, G. E. *J. Am. Chem. Soc.* **1983**, *105*, 3767.

(28) Janes, N.; Oldfield, E. *J. Am. Chem. Soc.* **1985**, *107*, 6769.

(29) Harris, R. K.; Kennedy, J. D.; McFarlane, W. In *NMR and the Periodic Table*; Harris, R. K., Mann, B. E., Eds.; Academic: New York, 1978; Chapter 10.

(30) Harris, R. K.; Knight, C. T. G.; Hull, W. E. *J. Am. Chem. Soc.* **1981**, *103*, 1577.

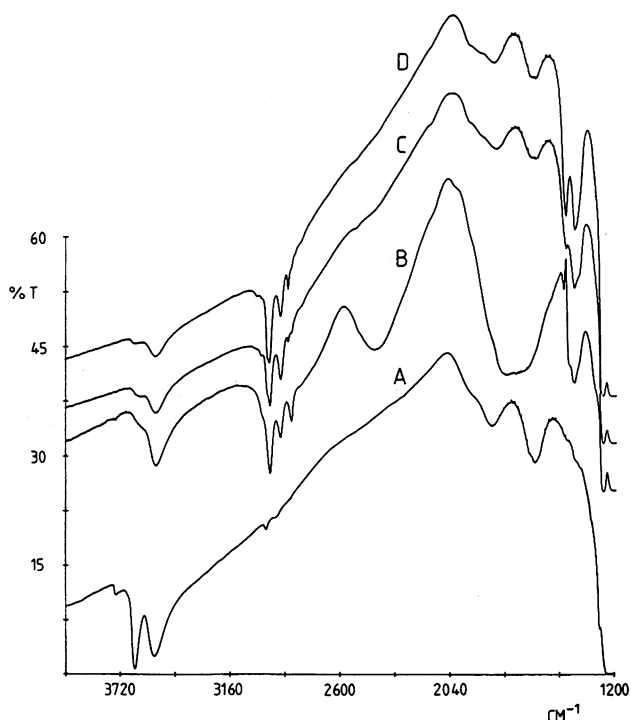
(31) Marsmann, H. C.; Meyer, E.; Vongehr, M.; Weber, E. F. *Makromol. Chem.* **1983**, *184*, 1817.

(32) Magi, M.; Lippmaa, E.; Samosan, A.; Englehardt, G.; Grimmer, A.-R. *J. Phys. Chem.* **1984**, *88*, 1518.

(33) Ramdas, S.; Klinowski, J. *Nature (London)* **1984**, *308*, 521.

**Table II.**  $^{29}\text{Si}$  CP-MAS Resonances Observed after Adsorption of Trimethylmethoxysilane ( $\text{Me}_3\text{SiOMe}$ ) on HY Zeolite

conditions	assignment	shift, ppm	mol %
vapor 295 K, 120 min, degassed 30 min	Lewis adduct	31	17
	$\text{Me}_3\text{SiOMe}$	20	45
	$\text{Me}_3\text{SiOSi}$	10	38
degassed 403 K, 180 min	$\text{Me}_2\text{Si}(\text{OMe})_2$	0	28
	$\text{Me}_2\text{Si}(\text{OMe})\text{OSi}$	-11	54
	$\text{Me}_2\text{Si}(\text{OSi})_2$	-20	18
degassed 523 K, 12 h	$\text{Me}_2\text{Si}(\text{OMe})_2$	0	55
	$\text{Me}_2\text{Si}(\text{OMe})\text{OSi}$	-11	
	$\text{Me}_2\text{Si}(\text{OSi})_2$	-20	
	$\text{MeSi}(\text{OMe})(\text{OSi})_2$	-56	
	$\text{Me}_2\text{Si}(\text{OMe})_2$	2	
vapor 473 K, 120 min, degassed 10 min	$\text{Me}_2\text{Si}(\text{OMe})_2$	2	18
	$\text{Me}_2\text{Si}(\text{OSi})_2$	-19	32
	$\text{MeSi}(\text{OMe})_2\text{OSi}$	-39	9
	$\text{MeSi}(\text{OMe})(\text{OSi})_2$	-57	41

**Figure 2.** IR spectra of wafer of HY zeolite, degassed at 670 K, loaded with  $\text{Me}_3\text{SiOMe}$ : (A) the degassed zeolite; (B) equilibrated for 10 min at 295 K, degassed for 30 min; (C) equilibrated for 60 min at 403 K, degassed for 10 min; and (D) equilibrated for 120 min at 473 K, degassed for 10 min.

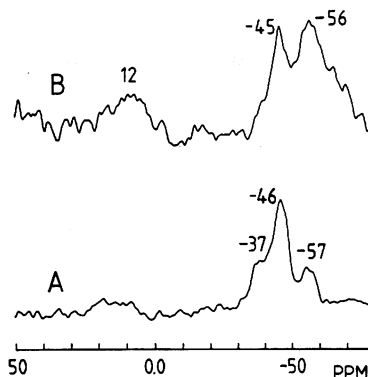
Trimethylsilyl groups bonded to the surface,  $\text{Me}_3\text{SiOSi}$ , are observed at 10 ppm (38%). The third peak at 31 ppm appears at an unusual position for oxygen-bonded silicon and will be labeled as a yet undefined Si-zeolite Lewis acid adduct (see below).

Upon degassing this material at 403 K under vacuum, striking changes occur in the  $^{29}\text{Si}$  NMR spectrum. None of the original silanes seen between 30 and 10 ppm survive this treatment, and new resonances at 0 (28%), -11 (54%), and -20 ppm (18%) are observed (Figure 1B). These data are consistent with the generation of  $\text{Me}_2\text{Si}(\text{OMe})_2$  (-2 ppm) and two products of condensation with the zeolite hydroxyls:  $\text{Me}_2\text{Si}(\text{OMe})\text{OSi}$  and  $\text{Me}_2\text{Si}(\text{OSi})_2$  (Table II).

Further heating at higher temperature (523 K) causes further condensation of the dimethylsiloxane species (Figure 1C).

If dehydrated HY is equilibrated with vapor of  $\text{Me}_3\text{SiOMe}$  at 473 K, more pronounced condensation is observed compared to the vacuum treatments (Figure 1D).

The IR spectrum of a self-supporting wafer of  $\text{NH}_4\text{Y}$  zeolite, degassed at 670 K for 14 h under vacuum, is shown in Figure 2A. Three well-known hydroxyl groups can be distinguished: terminal Si-OH groups at the outer surface of the zeolite crystals (3740  $\text{cm}^{-1}$ ), "supercage"  $\text{SiO}(\text{H})\text{Al}$  hydroxyls at 3640, and "sodalite"

**Figure 3.**  $^{29}\text{Si}$  CP-MAS NMR spectra of methyltrimethoxysilane chemisorbed on dehydrated HY zeolite: (A) equilibrated for 120 min at 295 K, degassed for 30 min (0.3/SC); and (B) degassed at 403 K for 180 min (<0.1/SC).**Table III.**  $^{29}\text{Si}$  CP-MAS Resonances Observed after Adsorption of Methyltrimethoxysilane ( $\text{MeSi}(\text{OMe})_3$ ) on HY Zeolite

conditions	assignment	shift	mol %
vapor 295 K, 10 min, degassed 30 min	$\text{Me}_3\text{SiOMe}$	18	7
	$\text{Me}_3\text{SiOSi}$	8	7
	$\text{MeSi}(\text{OMe})_3$	-37	14
	$\text{MeSi}(\text{OMe})_2\text{OSi}$	-46	53
degassed 403 K, 180 min	$\text{MeSi}(\text{OMe})(\text{OSi})_2$	-57	19
	$\text{Me}_3\text{SiOSi}$	12	22
	$\text{MeSi}(\text{OMe})_2\text{OSi}$	-45	25
	$\text{MeSi}(\text{OMe})(\text{OSi})_2$	-56	53

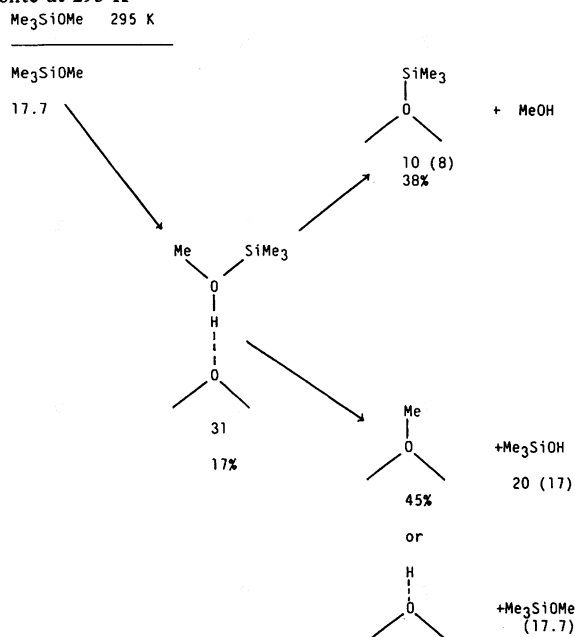
$\text{SiO}(\text{H})\text{Al}$  at 3540  $\text{cm}^{-1}$ . The latter two species, depicted as  $\text{SiO}(\text{H})\text{Al}$  or HOZ, are bridged hydroxyls, located in different framework positions in the Si-O-Al six-rings of the faujasite structure.

If the zeolite wafer is equilibrated with vapor of  $\text{Me}_3\text{SiOMe}$  and pumped off for 30 min, striking changes in the spectrum indicate an acid-base reaction between the zeolite hydroxyls and the silane (Figure 2B). The high-frequency supercage hydroxyls are almost entirely consumed upon chemisorption, whereas the low-frequency hydroxyls are essentially unaffected. In addition to the expected C-H stretching and bending vibrations of the silane (3000-2800 and 1480-1370  $\text{cm}^{-1}$ ), two strong broad bands are observed at 2425 and 1750  $\text{cm}^{-1}$ . The former vibration is assigned to proton-stretching modes of protonated siloxane species, like  $\text{Me}_2\text{SiOH}-\text{OT}_2$ , that are protolysis products of the chemisorbed silane. The band around 1750  $\text{cm}^{-1}$  cannot be correlated to a specific species at the present time. The spectroscopic observations and their interpretations are summarized in Scheme I.

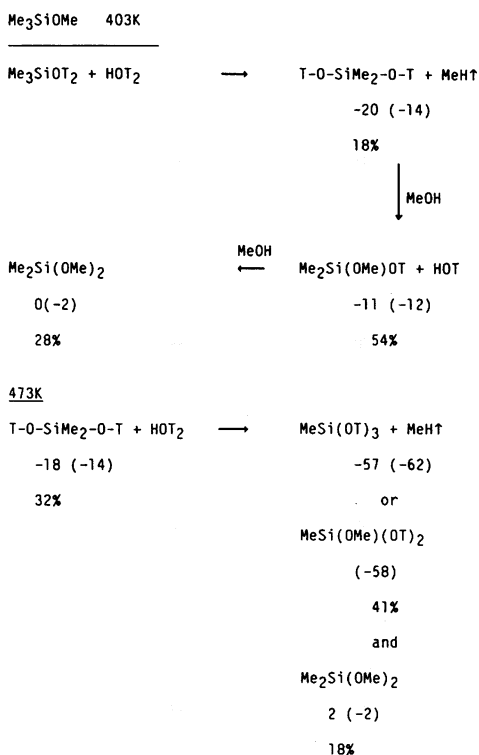
Treatment of the zeolite wafer with silane at 403 K for 1 h results in dramatic changes (Figure 2C). In addition to the supercage hydroxyls, a large fraction of the previously inaccessible low-frequency hydroxyls are also consumed. The broad bands at 1750 and 2425  $\text{cm}^{-1}$  are destroyed, and changes in the C-H stretch intensities at 2860  $\text{cm}^{-1}$  indicate the loss of certain species. Further treatment with silane vapor at elevated temperature (2 h at 473 K) causes continued consumption of the hydroxyl groups and formation of a new species at 1455  $\text{cm}^{-1}$  (Figure 2D). This mode is assigned to the methoxy group of the trisubstituted, framework anchored siloxane  $\text{MeSi}(\text{OMe})(\text{OSi})_2$  which is observed in the corresponding NMR experiment (Figure 1D).

Heating at elevated temperatures removes the unstable products and intermediates from the zeolite. None of the previous species remain, and the NMR data allow the conclusion that di- and trisubstituted siloxanes are formed (Scheme II). Additional protons are delivered from nonaccessible sites into the supercage, as indicated by IR spectroscopy. At this stage, methyl groups are split off from the silane. This behavior is unknown with silica supports and points to the strong acidity of the zeolite. One reaction path proposed is the acid-catalyzed methyl-group substitution at the framework bonded monosiloxane (Scheme II). At higher degassing temperatures (523 K), the higher condensation



**Scheme I.** Proposed Reaction Pathways for Me<sub>3</sub>SiOMe in HY Zeolite at 295 K<sup>a</sup>

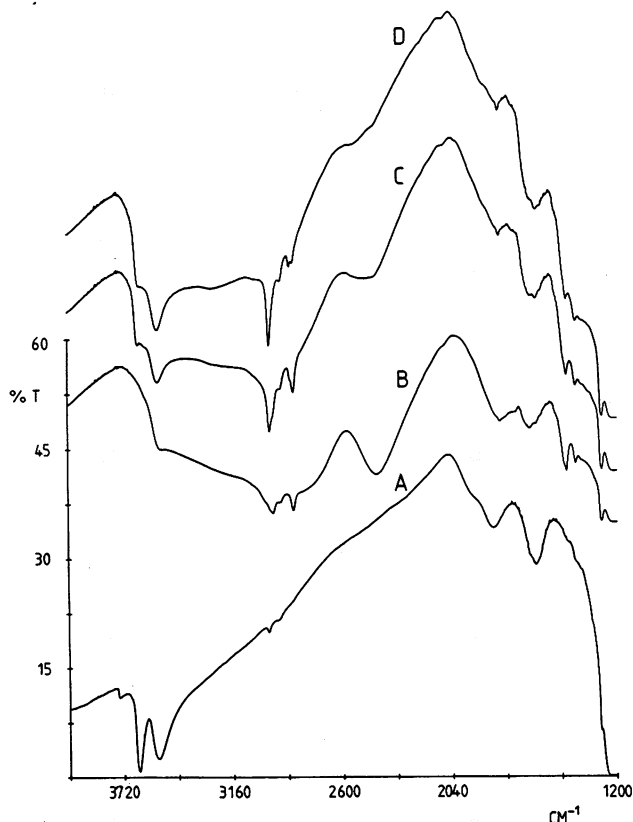
<sup>a</sup> Indicated values are the <sup>29</sup>Si chemical shift data, compared to expected values (Table I) in parentheses. Percent values refer to the relative amounts of silane species as detected by <sup>29</sup>Si MAS-NMR.

**Scheme II.** Proposed Reaction Pathways for Me<sub>3</sub>SiOMe in HY Zeolite at Elevated Temperatures

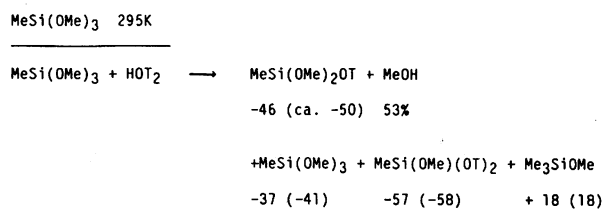
product Me<sub>2</sub>Si(OSi)<sub>2</sub> becomes more pronounced, and an additional trisubstituted species MeSi(OSi)<sub>3</sub> grows in.

**Methyltrimethoxysilane.** At least four new silicon species are observed in the <sup>29</sup>Si NMR of HY upon equilibration with MeSi(OMe)<sub>3</sub> at 295 K. New peaks appear at 18, 8, -37, -46, and -57 ppm (Figure 3A). These observations, with corresponding assignments, are summarized in Table III and in Scheme III.

The major component of the spectrum at -46 ppm (53%) can be assigned to the monosubstituted starting silane, MeSi(OMe)<sub>2</sub>OSi. The resonance at -57 ppm is due to disubstituted product, MeSi(OMe)(OSi)<sub>2</sub>.



**Figure 4.** IR spectra of a wafer of HY zeolite, degassed at 670 K, loaded with MeSi(OMe)<sub>3</sub>: (A) the degassed zeolite; (B) equilibrated for 10 min at 295 K, degassed for 30 min; (C) equilibrated for 60 min at 403 K, degassed for 10 min; and (D) equilibrated for 120 min at 473 K, degassed for 10 min.

**Scheme III.** Proposed Reaction Pathways for MeSi(OMe)<sub>3</sub> in HY Zeolite at 295 K

Upon degassing this material at 403 K under vacuum, a gradual shift of intensities in favor of the higher condensation products is observed (Figure 3B). The heat treatment transforms the major fraction of the silane into methoxymethylsilyl groups, MeSi(OMe)(OSi)<sub>2</sub>, at -56 ppm (53%), in addition to MeSi(OMe)<sub>2</sub>(OSi).

Saturation of the dehydrated zeolite wafer (Figure 4A) with MeSi(OMe)<sub>3</sub> at 295 K causes dramatic changes in the IR spectrum. An extremely strong and broad absorption appears between 3600 and 2600 cm<sup>-1</sup> (Figure 4B). The only structure visible on this absorption is a shoulder at 3525 (sodalite hydroxyl) and the C-H stretch bands at 3000-2800 cm<sup>-1</sup>. The broad absorption is assigned to a convolution of free hydroxyl and intermolecular bonded hydroxyl vibrations, most likely due to interactions of the byproduct MeOH with the zeolite hydroxyls. At 2425 cm<sup>-1</sup>, a strong, symmetric absorption appears that is assigned to weaker hydroxyl bonds with the starting material, as observed with Me<sub>3</sub>SiOMe (Figure 2).

It should be noted that hydrolyzable groups at silanes do not always lead to a complete consumption of zeolite hydroxyls. At elevated temperatures, only the monomethoxysilane Me<sub>3</sub>SiOMe shows an increasing tendency to destroy the inaccessible "sodalite" protons, whereas Me<sub>3</sub>SiCl and MeSi(OMe)<sub>3</sub> leave these groups essentially unaffected.

**Table IV.**  $^{29}\text{Si}$  CP-MAS Resonances Observed after Adsorption of Trimethylchlorosilane ( $\text{Me}_3\text{SiCl}$ ) on HY and NaY Zeolites

conditions	assignment	shift	mol %
HY			
vapor 295 K, 120 min, degassed 30 min	Lewis adduct	40	17
	$\text{Me}_3\text{SiOH}$	21	42
degassed 403 K, 180 min	$\text{Me}_3\text{SiOSi}$	12	24
	$\text{Me}_2\text{Si}(\text{OH})\text{OSi}$	-5, -10	17
	Lewis adduct	41	10
	$\text{Me}_3\text{SiCl}$	27	46
	$\text{Me}_3\text{SiOH}$	21	
	$\text{Me}_3\text{SiOSi}$	13	
vapor 473 K, 120 min, degassed 30 min	$\text{Me}_2\text{Si}(\text{OH})\text{OSi}$	-9	28
	$\text{MeSi}(\text{OH})(\text{OSi})_2$	-50	16
	$\text{Me}_3\text{SiOSi}$	7	37
	$\text{Me}_2\text{Si}(\text{OH})(\text{OSi})$	-11, -14	33
	$\text{MeSi}(\text{OH})(\text{OSi})_2$	-53	15
	$\text{MeSi}(\text{OSi})_3$	-59	15
NaY			
vapor 295 K, 120 min, degassed 30 min	Lewis adduct	38	77
	$\text{Me}_3\text{SiOH}$	18	14
	$\text{Me}_3\text{SiOSi}$	6	9

The reactions of the trimethoxysilane can be understood in terms of protolysis and condensation with the framework, as summarized in Scheme III. Reaction of the methoxy groups with zeolite protons causes breaking of the oxygen-silicon bond to give framework bonded siloxanes and methanol (Scheme III). The methanol hydroxyls are detected in corresponding IR spectra (Figure 4B). As with  $\text{Me}_3\text{SiOMe}$ , the chemisorption of the trimethoxysilane in acid zeolite proves to be irreversible: Supercage hydroxyls are not restored at higher degassing temperatures (Figure 4C,D), indicating that stoichiometric substitution reactions take place, rather than acid-catalyzed hydrolysis of the adsorbed silane.

**Trimethylchlorosilane.** Saturation of HY with vapor of  $\text{Me}_3\text{SiCl}$  at 295 K generates four new silicon species in the  $^{29}\text{Si}$  NMR of the zeolite (Table IV, Figure 5A). The component at 21 ppm (42%) is assigned to  $\text{Me}_3\text{SiOH}$  (predicted 17 ppm). The resonance at 12 ppm (24%) is assigned to trimethylsiloxy groups and the broad resonance between -5 and -10 ppm to dimethylsiloxy groups, both bonded to the zeolite.

The sample also exhibits a peak at +40 ppm (17%). In addition to  $\text{Me}_3\text{SiCl}$ -treated zeolites, several other of the materials studied here exhibit a peak at about +40 ppm.

Several observations regarding this resonance are summarized below.

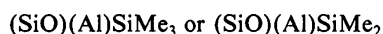
(a) Resonances with comparable chemical shift are observed after exposure to  $\text{Me}_3\text{SiH}$  (41 ppm),  $(\text{Me}_3\text{Si})_2\text{NH}$  (41 ppm),  $\text{Me}_3\text{SiOMe}$  (31 ppm), and  $\text{Me}_3\text{SiCl}$  (40 ppm) but are not formed from  $\text{MeSi}(\text{OMe})_3$ . This suggests that the species is a *substituted trimethylsilyl group*.

(b)  $^{29}\text{Si}$  chemical shift correlations reported earlier<sup>28</sup> allow us to exclude the presence of a  $\pi$ -bonding, electronegative ligand on Si, as this would move the chemical shift upfield into the range encompassed by the species listed in Table I. In fact, no tetravalent silanes or siloxanes having H, Cl, Me, or OMe ligands exhibit shifts this far to low field.

(c) These same chemical shift correlations predict that a ligand which has higher electronegativity than Me and which is capable of only  $\sigma$ -bonding, and not  $\pi$ -bonding interactions with Si, will produce a downfield shift like that observed. Indeed, trimethylsilyl ligands on metals are known to exhibit chemical shifts above +35 ppm (e.g.,  $(\text{Me}_3\text{Si})_2\text{Hg}$ , +64 ppm).

These observations do not lead to a definite assignment for this resonance, but two possibilities are listed below.

(1) The first is a silane-Lewis acid adduct, with a direct Si-metal bond, like



This proposed species is also consistent with a proton-consuming reaction, which is indicated by the loss of intensity of zeolite hydroxyls in the IR spectra.

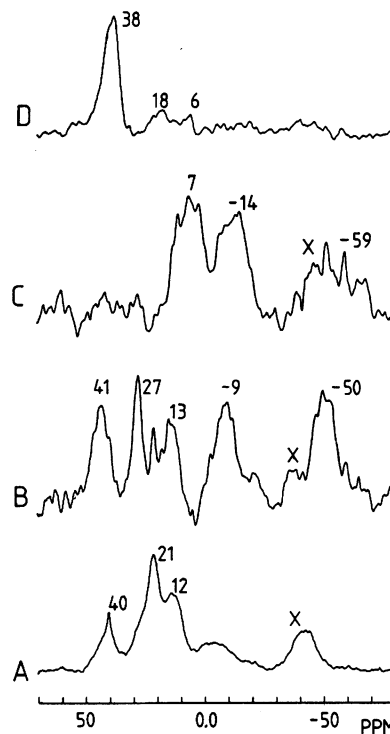
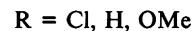
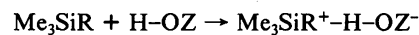


**Figure 5.**  $^{29}\text{Si}$  CP-MAS NMR spectra of trimethylchlorosilane chemisorbed on dehydrated HY zeolite. X denotes spinning sidebands from the zeolite framework resonances. (A) Equilibrated for 120 min at 295 K, degassed for 30 min (1.2/SC); (B) degassed for 180 min at 403 K (<0.2/SC); (C) equilibrated for 120 min at 473 K, degassed for 30 min (2.1/SC); and (D) dehydrated NaY zeolite, equilibrated with the silane at 295 K for 120 min, degassed for 30 min (2.8/SC).

(2) The second is reaction with acidic zeolite hydroxyls to form a strongly hydrogen-bonded silane, with partial positive charge on Si, as



Even though this species cannot be identified unambiguously in the present study, the authors favor the first alternative because the product is independent of the reactive group (Cl, OMe, etc.) at the silane.

If the  $\text{Me}_3\text{SiCl}/\text{HY}$  adduct is degassed at 403 K, higher substituted siloxane species (-9 ppm,  $\text{Me}_2\text{Si}(\text{OH})\text{OSi}$ ; -50 ppm,  $\text{MeSi}(\text{OH})(\text{OSi})_2$ ) are observed (Figure 5B). A more severe treatment of the zeolite with silane vapor at 473 K gives rise to a different product pattern (Figure 5C): The higher partial pressure of the starting material causes a high concentration of the framework-anchored  $\text{Me}_3\text{Si}(\text{OSi})$  at about 7 ppm (37%). Trisubstituted siloxanes are generated in substantial amounts under the high partial pressure conditions; species with resonances between -51 and -59 ppm (e.g.,  $\text{MeSi}(\text{OH})(\text{OSi})_2$ ) account for 30% of the silicon loading.

Chemisorption experiments with  $\text{Me}_3\text{SiCl}$  in non-acidic NaY support provide further evidence as to the nature of the acid reaction products (Figure 5D): The predominant species is a resonance at 38 ppm (77%), accompanied by smaller amounts of  $\text{Me}_3\text{SiOH}$  at 18 ppm and  $\text{Me}_3\text{Si}(\text{OSi})$  at 6 ppm. Since the chemical shift of  $\text{Me}_3\text{SiCl}$  is 30 ppm, the peak at 38 ppm is unlikely to represent the unreacted starting material. This species is proposed to be due to an association between the zeolite sodium ions and the silane.

If a dehydrated wafer of HY is equilibrated with  $\text{Me}_3\text{SiCl}$  at 295 K in the IR cell, a consumption of the major fraction of supercage hydroxyls is observed as with the other silanes under study (Figure 6B). A major difference to the former systems is the high-frequency band between 3500 and 3100  $\text{cm}^{-1}$ , indicating hydroxyl bridges of moderate strength. This band can be un-

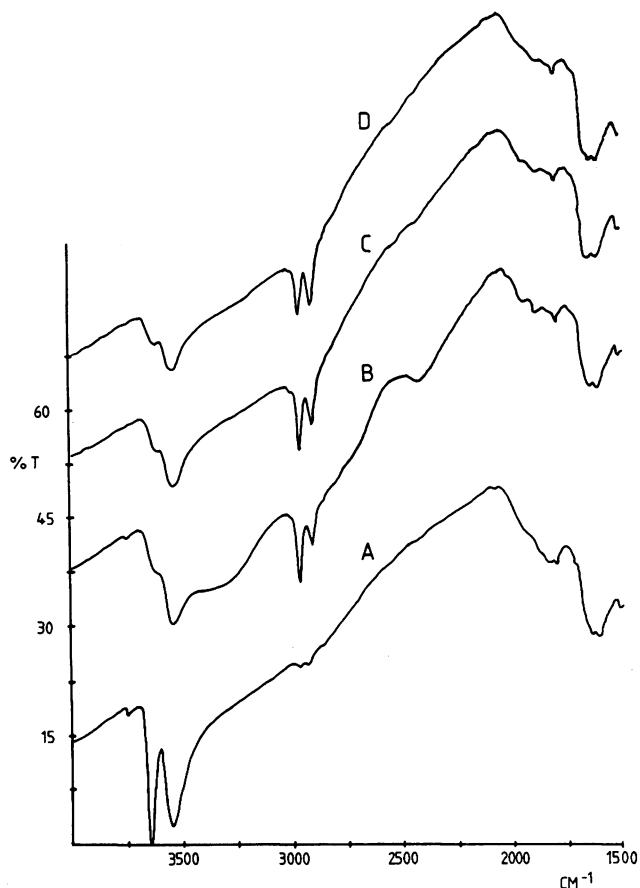


Figure 6. IR spectra of a wafer of HY zeolite, degassed at 670 K, loaded with  $\text{Me}_3\text{SiCl}$ : (A) the degassed zeolite; (B) equilibrated for 10 min at 295 K, degassed for 30 min; (C) equilibrated for 60 min at 403 K, degassed for 10 min; and (D) equilibrated for 120 min at 473 K, degassed for 10 min.

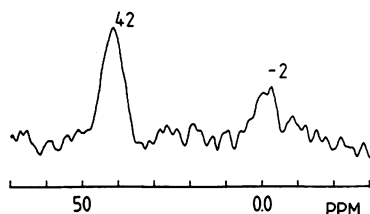


Figure 7.  $^{29}\text{Si}$  CP-MAS NMR spectrum of trimethylsilane equilibrated with dehydrated HY zeolite for 120 min at 473 K, degassed for 30 min (1.8/SC).

derstood as being due to a Si-Cl-H bridge in  $\text{Me}_3\text{SiCl}\cdots\text{HOZ}$ .

An additional hydrogen bond is represented by the band at  $2425\text{ cm}^{-1}$ . This band is found with *all* silanes studied. This suggests the formation of a common intermediate, probably with a Si-OH $\cdots$ OZ bond. Free  $\text{Me}_3\text{SiH}$  shows a  $\nu(\text{Si-H})$  at  $2125\text{ cm}^{-1}$ . No HCl ( $2885\text{ cm}^{-1}$ ) is detected in the IR of the gas phase equilibrated with the zeolite. The C-H stretching and bending ( $1410$  and  $1260\text{ cm}^{-1}$ ) frequencies resemble those of neat  $\text{Me}_3\text{SiCl}$ , indicating that the  $\text{Me}_3\text{Si}$  unit is intact.

Treatment of the zeolite wafer with silane at 403 K and degassing partially removes both the broad, bridged-hydroxyl band between  $3500$  and  $3100\text{ cm}^{-1}$  and the hydrogen band at  $2425\text{ cm}^{-1}$  (Figure 6C). This observation is indicative of increasing condensation reactions that are still more pronounced if the treatment is done at 473 K (Figure 6D). The proposed reaction pathways for  $\text{Me}_3\text{SiCl}$  in HY are summarized in Scheme IV.

**Trimethylsilane.** Dehydrated HY zeolite, equilibrated with  $\text{Me}_3\text{SiH}$  vapor at 295 K for 120 min, followed by evacuation for 30 min, exhibits no  $^{29}\text{Si}$  NMR signal in the silane or siloxane regions of the spectrum. The quantity of physisorbed silane is apparently too small to be detected in the  $^{29}\text{Si}$  NMR.

Scheme IV. Proposed Reaction Pathways for  $\text{Me}_3\text{SiCl}$  in HY Zeolite at (A) 295 K and (B) Elevated Temperatures

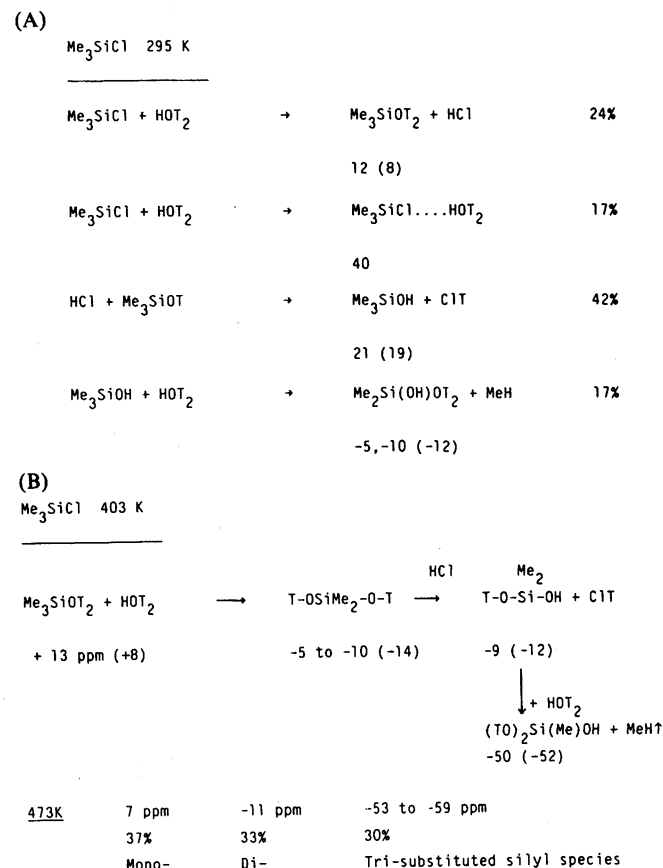


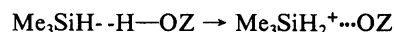
Table V.  $^{29}\text{Si}$  CP-MAS Resonances Observed after Adsorption of Trimethylsilane ( $\text{Me}_3\text{SiH}$ ) or Hexamethyldisilazane ( $(\text{Me}_3\text{Si})_2\text{NH}$ ) on HY Zeolite

conditions	assignment	shift	mol %
vapor 473 K, 120 min, degassed 30 min	$\text{Me}_3\text{SiH}$		
	Lewis adduct	41	60
	$\text{Me}_2\text{Si}(\text{OMe})_2$	-2	40
vapor 473 K, 120 min, degassed 30 min	$(\text{Me}_3\text{Si})_2\text{NH}$		
	Lewis adduct	41	38
	$\text{Me}_3\text{SiOSi}$	10	35
	$\text{Me}_2\text{Si}(\text{OSi})_2$	-14	27

If the silane treatment is carried out at 473 K, however, two distinct products are identified in the NMR (Table V, Figure 7). The major product is found at +41 ppm (60%). A second species at -2 ppm is due to  $\text{Me}_4\text{Si}$  or  $\text{Me}_2\text{Si}(\text{OMe})_2$ .

A dehydrated wafer of HY (Figure 8A) shows formation of a hydroxyl bond with  $\text{Me}_3\text{SiH}$  if equilibrated at 295 K (Figure 8B). The spectrum also shows a splitting of the Si-H vibration (gas phase  $2125\text{ cm}^{-1}$ ) into modes at  $2050$  and  $2125\text{ cm}^{-1}$ , as well as a weaker band at about  $2425\text{ cm}^{-1}$ .

The high-frequency zeolite hydroxyl band at  $3640\text{ cm}^{-1}$  is reduced to a shoulder, and a broad band between  $3500$  and  $3200\text{ cm}^{-1}$  indicates a hydroxyl bridge with the adsorbed silane. This hydroxyl bridge is believed to generate the low-frequency part of the  $\nu(\text{Si-H})$  vibration at  $2050\text{ cm}^{-1}$  by forming a trimethylsilylium ion:



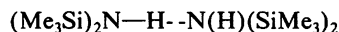
The broadening of both the  $2050$ - and  $2125\text{-cm}^{-1}$  bands indicates strong absorption on the zeolite surface. Silylium ions have been observed in the gas phase by ion cyclotron resonance.<sup>34</sup>



of dehydrated HY (Figure 10A) is saturated with the silazane, almost *no* interaction with the zeolitic hydroxyls at 3640 and 3540  $\text{cm}^{-1}$ , except the terminal SiOH at 3745  $\text{cm}^{-1}$ , is detected (Figure 10B). This is in strong contrast to all other silanes studied. A new high-frequency band at 3400  $\text{cm}^{-1}$  is assigned to the  $\nu(\text{N-H})$  and the broad bands at 1500–1400  $\text{cm}^{-1}$  to the corresponding N–H bending vibrations. A very broad absorption between 3400 and 2400  $\text{cm}^{-1}$  is due to intermolecular N–H hydrogen bridges. Hydroxyl bridges can be excluded since the zeolite hydroxyls remain unaffected by the chemisorption.

If the zeolite wafer is saturated with silazane again at 403 K, *both* zeolite hydroxyl bands now are almost completely destroyed (Figure 10C), indicating that sodalite protons have traveled into the supercage. The  $\nu(\text{N-H})$  band at 3400  $\text{cm}^{-1}$  is significantly diminished, due to reaction with the zeolite hydroxyls. A strong broad band at 1430  $\text{cm}^{-1}$  is assigned to ammonium ions formed upon protonation by the acid zeolite. The  $\delta(\text{C-H})$  band at 1260  $\text{cm}^{-1}$  (due to  $\text{CH}_3\text{Si}$ ) grows significantly upon vapor treatment at 403 K. This provides evidence for the anchoring reaction as indicated by the NMR results. Silazane treatment at 473 K pronounces the reactions observed at 403 K (Figure 10D).

The reactivity of  $(\text{Me}_3\text{Si})_2\text{NH}$  in acid Y zeolite is lower than that of methoxy- and chlorosilanes. This is shown in the in situ IR by the intact zeolite hydroxyls after adsorption at 295 K. Strong intermolecular N–H bridges characterize the intrazeolite environment of the silazane:



At elevated temperatures, the zeolite hydroxyls do react almost to completion with the silazane, generating several protolysis products. NMR and IR data are consistent with the anchoring reactions outlined in Scheme V.

### Conclusion

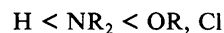
The reactivity of functionalized silanes with the bridged hydroxyls within zeolitic pore systems has been investigated employing a combination of  $^{29}\text{Si}$  solid-state NMR and in situ IR techniques.

Due to their extreme acidity, the bridged zeolitic hydroxyls react in a fashion strikingly different from the behavior of terminal hydroxyls found at the surface of amorphous oxides. At moderate temperature, functional groups at the silane like OR, Cl,  $\text{NR}_2$ ,

or H are lost to form bridges to the zeolite framework. The reaction does not stop at this point, however. Si–C bonds are broken at elevated temperature, splitting off alkyl groups, and more highly substituted siloxane species are anchored to the framework.

The incorporation of silyl groups into the zeolite lattice could be considered as a model for early steps during the more severe lattice rearrangements observed upon reacting  $\text{SiCl}_4$  with an acid zeolite. In the latter case, framework aluminum atoms are substituted by silicon.

On the basis of the number of products and the reversibility of silane chemisorption, the reactivity of functional groups at Si with bridged zeolitic hydroxyls increases in the sequence



If  $\text{Me}_3\text{Si-H}$ ,  $-\text{NR}_2$  or  $-\text{Cl}$  is reacted with the acidic zeolite, a product with a very unusual  $^{29}\text{Si}$  chemical shift at about +40 ppm is observed. Although no definitive assignment for this species can be given at this time, it is clear that an electronegative  $\sigma$ -bonding ligand must be bonded to Si. The observations indicate either a strongly hydrogen-bonded silane with partial positive charge on the Si or a silane–Lewis acid adduct, incorporated into the framework with a direct Si–metal bond.

Despite the complexity of the reactions considered, it is clear that bridged hydroxyls on solid surfaces are far more reactive than terminal hydroxyls.

The results of this study provide the basis for a systematic approach to modify and “functionalize” the internal surface of zeolitic cage systems. The work has been extended to reactive phosphorus compounds,<sup>36</sup> and related results will be reported elsewhere.

**Acknowledgment.** The technical assistance of M. P. Stepro and D. E. Rothfuss is appreciated. The authors gratefully acknowledge discussions with Dr. D. B. Chase (DuPont), C. A. Fyfe (Guelph), and L. Baltusis (Varian).

**Registry No.**  $\text{Me}_3\text{SiOMe}$ , 1825-61-2;  $\text{MeSi(OMe)}_3$ , 1185-55-3;  $\text{Me}_3\text{SiCl}$ , 75-77-4;  $\text{Me}_3\text{SiH}$ , 993-07-7;  $(\text{Me}_3\text{Si})_2\text{NH}$ , 999-97-3.

(36) Bein, T.; Chase, D. B.; Farlee, R. D.; Stucky, G. D. Proceedings of the 7th International Zeolite Conference, Tokyo, 1986; Murakami, Y., Iijima, A., Ward, J. W. Eds.; Kodansha: Tokyo, 1986; p 311.